Imaging by silicon on insulator waveguides

Q. Song,[a] F. Qian, E. K. Tien, I. Tomov, J. Meyer, X. Z. Sang, and O. Boyraz
Department of Electrical Engineering and Computer Science, Advanced Photonics Device and System Laboratory, UC Irvine, Irvine, California 92697, USA

(Received 26 January 2009; accepted 1 May 2009; published online 8 June 2009)

We present multiphoton imaging based on semiconductor planar waveguide technology which can be used as a transmitter and receiver simultaneously. In particular, silicon on insulator waveguides with *p-i-n* diode structures are used to demonstrate <5 μm resolution three-photon imaging of $Er^{3+}:Y_2O_3$ microparticles by using 1550 nm excitation. Additional theoretical study has been performed to demonstrate the proposed scheme for three-dimensional tomography of micron-sized objects, which could be realized by using multiple transmitter-detector pairs. © *2009 American Institute of Physics*. [DOI: 10.1063/1.3141480]

Fluorescence imaging is an effective tool of biological and nonbiological sciences. Over the past decades, several fluorescence based optical imaging techniques have been proposed and demonstrated. In particular, wide-field microscopy with up to 0.6 μm resolution,[1] confocal microscopy with up to 200 nm resolution,[2–4] and multiphoton microscopy[5] have been widely utilized in biological sciences to deliver two-dimensional and three-dimensional (3D) imaging. Conventional multiphoton microscopes consist of a light source, the optical focus part and image detector to generate point by point imaging. Hence, a high numerical aperture (NA) objective lens is the most essential component to confine light in a small volume to produce high intensity and high resolution imaging. The resolution and imaging quality ultimately are determined by the objective lens and hence the diffraction limit. Also, the image detector needs to be separately assembled in free space and it is voluminous.[6]

Silicon-on-insulator (SOI)-based planar waveguide technology is the chip scale counterpart of high numerical aperture lenses. Because of the large index contrast between the core ($n\sim3.45$) and the cladding ($n\sim1.5$), SOI waveguides can deliver tight mode confinement along the waveguide, and hence it attracted many researchers to illustrate chip scaled nonlinear optical devices.[7–10] In this paper, we propose an idea that utilizes SOI waveguides as a high NA objective lens (NA$\sim$3.10) to deliver well focused infrared beam and to excite multiphoton fluorescence, and the waveguide facet as an embedded *p-i-n* receiver with less than 0.01 A/W responsivity to provide imaging. Experimentally we demonstrate multiphoton imaging of $Er^{3+}:Y_2O_3$ microparticles with 5 μm resolution by using 1550 nm excitation. The size of the waveguide determined the resolution of the system. Theoretical study has been performed to illustrate potential use of the proposed scheme for tomography of micron-sized cell-like objects, which could be realized by using multiple transmitter–detector pairs.[2]

To use the same waveguide as a transmitter and a receiver, the material should be transparent at the excitation wavelength and absorbing at the fluorescence wavelength. Silicon is transparent at wavelengths above 1.1 μm and it is a good candidate for infrared excitation. Also, silicon is an absorbing media from 0.2 to 1.1 μm and it is widely used in that wavelength range as a photodetector.[4] Using SOI-based planar waveguide technology, silicon can simultaneously be utilized to deliver tightly confined optical beam on fluorescent particles, and to detect multiphoton fluorescence by using the facet of the waveguide, as shown in Fig. 1. Here, unlike a conventional *p-i-n* detector, the intrinsic region is sandwiched laterally in between two doped regions and provide vertical detection surface. Experimentally, we use an SOI waveguide with 5 μm^2 modal area to illustrate the SOI-based multiphoton imaging. The total area between *pn* junctions is $\sim$25 μm^2, which determines the total detection area, as shown in Fig. 1. Since multiphoton fluorescence is intensity dependent and it is at maximum when there is a full overlap between beam and the particle, we can use the fluorescence intensity as a means to monitor beam particle overlap, and to determine the external boundaries of the particle. The resolution here is determined by the mode diameter in the image plane. The detection surface, on the other hand, is related to the collection efficiency and it will not influence the resolution. The detector responsivity is measured to be lower than 0.01 A/W by using a 632 nm light source before imaging. The low responsivity is mainly due to the fact that *pn* junctions do not extend until the front facet, and cause poor electrical efficiency.

Figure 2 illustrates the experimental setup used to demonstrate multiphoton imaging. To generate multiphoton fluorescence, we use erbium doped Y_2O_3 glass particles as a target object placed $\sim$5 μm away from the waveguide facet. Although the size of the particle used in the experiment can-

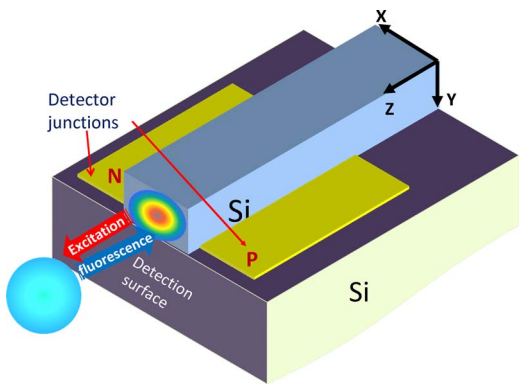

FIG. 1. (Color online) The 3D view of *p-i-n* junction waveguide.

[a]Electronic mail: unlogical0327@yahoo.com.cn.

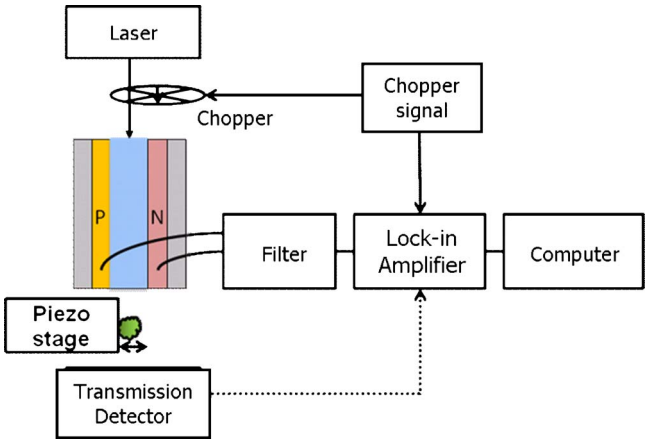

FIG. 2. (Color online) The imaging acquisition system of erbium doped fluorescent particle. Photocurrent is sent to the filtered amplifier and the computer. The silicon waveguide and external photodiode are switchable in the circuit.

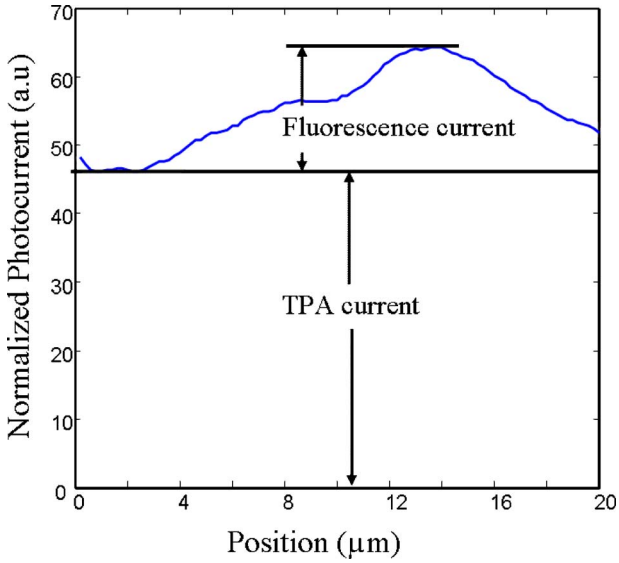

FIG. 3. (Color online) One of the fluorescence current lines extracted from the raw image.

not be precisely determined, a conventional microscope measurement shows that the particle size is smaller than 5 μm when they are compared to the known waveguide geometry placed in the same plane. The 1550 nm laser beam modulated by a mechanical chopper at 400 Hz is delivered on the sample by a 1 cm long silicon waveguide with 5 μm^2 mode size. The excitation by a 1550 nm pump laser used here produces three-photon fluorescence at 540 nm in $Er^{3+}:Y_2O_3$ particles by the cooperative upconversion process. The generated fluorescence in backward direction is then collected by the same waveguide facet. In this experiment we use the detector in the photovoltaic mode to avoid the noises originated from the biasing.[11] The detected photon current is measured by a lock-in amplifier. The signal is then sent to a computer to record for imaging. The image is obtained by moving the sample on a piezo actuated stage with 200 nm scanning steps in *x-y* plane (Fig. 1).

The total current flows through the electrical detection part could be described as[12]

$$I = I_L - I_0\left[\exp\left(\frac{e * IR_S}{nkT}\right) - 1\right] - \frac{IR_S}{R_{\text{load}}},$$

where I is the current flow through the lock-in amplifier, I_L is the photocurrent current generated by *p-i-n* diode, I_0 is diode reverse saturation current, R_{load} is the load resistance from the photodetector, R_S is the impedance of the electrical filter and amplifier, and n is the characteristic parameter of the diode. Under the photovoltaic mode, the junction is reversely biased by the voltage of IR_S. The photocurrent I_L generated by the waveguide detector consists of three components: the current generated by the pump laser due to two photon absorption (TPA), which has a large dc component and a random component, ambient noise, and the desired current generated by the fluorescence. Figure 3 illustrates an example of the measured current, and indicates the relative strength of the TPA current, which is $\sim 2/3$ of the total current. In order to create fluorescence image, we need to retrieve fluorescence current from the total photo current. Although the TPA efficiency is low for the power levels used in the experiment (<10 mW), the aggregate TPA current generated in 1 cm interaction length can be three times larger than the actual fluorescence current. Since the dc part of the TPA current is constant, its effect can be corrected digitally as part of the post processing. However, the dynamic range of the detector is reduced due to the presence of the TPA current. The background noise should also be minimized by shielding the experimental setup.

Figure 4(a) illustrates the image of a fluorescent particle captured by the SOI waveguide within 20 μm^2 scan area.

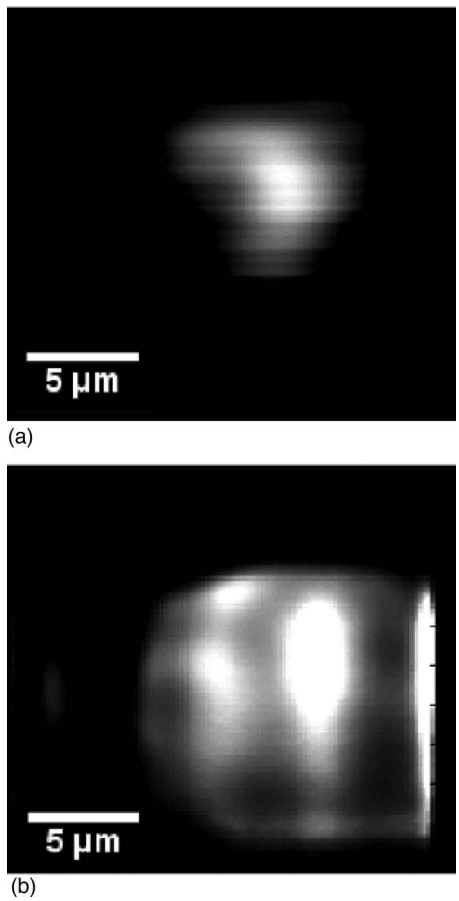

FIG. 4. (a) The 20×20 μm^2 fluorescent image from photocurrent by silicon waveguide. (b) The 20×20 μm^2 fluorescent image retrieved from photocurrent by external silicon diode.

The background TPA current is removed by subtracting dc level of the signal. The raw image is then deconvolved with the measured point spread function to generate the final image. Here, the point spread function of the waveguide is measured by 200 nm resolution raster scan of the radiation pattern by using a commercially available tapered fiber with 2 μm spot size. We obtain spreading diameter of 5 μm at the image plane. Therefore, the particle image shown on Fig. 4(a) is the point spread function of the waveguide imaging. This implies that the lateral resolution of the demonstrated imaging is close to 5 μm, which is mainly determined by the point spread function, and hence the dimensions of waveguide. Sharper resolution can be achieved by using submicron waveguide dimensions, which can give <0.1 μm^2 spot sizes and narrower point spread functions. However, the working distance will decrease due to diffraction and larger optical input power will be required to compensate nonlinear losses in small core waveguides. The detector geometry can also be optimized for the detection efficiency by adjusting parameters such as the *pn* junction separation. Additionally, the current waveguide design has ~ 1 cm *pn* junctions along the waveguide, which collects all the TPA current accumulated in the whole waveguide, and do not extend exactly up to the waveguide facet. Fabrication of *p-i-n* diodes just at the tip of the waveguide will both eliminate TPA current and increase the responsivity of the detector.

In addition to the beam size, the detection efficiency may also influence the resolution and image contrast. To assess the effect of the detector sensitivity, we image a similar particle by using a waveguide excitation and an external commercial detector with 0.3 A/W responsivity in the experimental setup, Fig. 2. Figure 4(b) shows the image generated by scanning a 20 μm^2 area and collecting the fluorescence by using an external photo detector. As expected, the absence of the TPA current and the larger active area with better sensitivity increase the image contrast. The large separation between the waveguide and the detector (>500 μm) results in collection of scattered light and produce blurred images, which cannot be corrected without a complex deconvolution process.[13,14] As the results indicate, two detection systems produce imaging with similar resolution after deconvolution process, and the resolution is limited by the point spread function in both cases. However, waveguide detection can be attractive when chip scale imaging is desired.

Based on the feasibility of multiphoton fluorescent planar imaging technology demonstrated above, prospective applications have been evaluated theoretically. In particular the performance of a planar imaging in a tomographic configuration has been estimated numerically. Figure 5(a) illustrates the simplified configuration used in our calculations. The simulations include multiple antennas (waveguides in this application) used as transmitters and receivers with fan shaped excitation beam.[2–15] The sample is a phantom object similar to the biological cell with two round objects inside, which is placed in the center of the platform surrounded by waveguides. In particular, we evaluate the resolution with respect to the number of transmitters and receivers pair. Figure 5(b) illustrates the reconstruction of object image, which is implemented based on scattering by using 36 transmitters. In this trial, only one transmitter is turned on at a time and

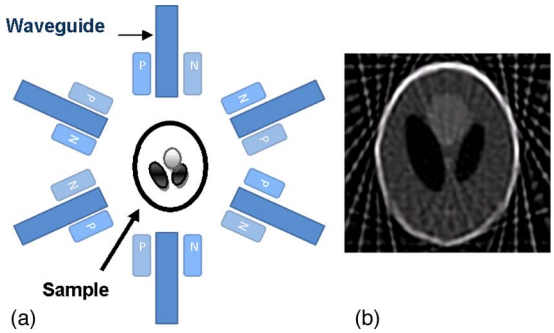

FIG. 5. (Color online) (a) The schematics of chamber with *pn* junctions addressed aside to six waveguides. (b) The reconstruction image of cell-like structure objects from simulation.

the image is constructed based on received radiation intensity by other receivers. Number of transmitters is increased until 1 μm resolution is achievable. These results indicate that 3D tomographic image of micron-sized particles can be obtained in a planar geometry by using multiple transmitter and receiver pairs from diverse incident angles. Although excitation mechanism will differ in multiphoton imaging, the radiation is similar to the scattering. Further study will be performed to determine achievable resolution in true multi photon imaging case.

In summary, we have first demonstrated that the SOI-based planar waveguide technology can effectively combine transmitter and detector together in multiphoton microscopy imaging. Imaging of micron-sized Er^{3+} particles is performed by using silicon waveguides and 1550 nm excitation. The 540 nm fluorescent images have been restored from the silicon waveguide with the *p-i-n* junction structure under photovoltaic mode. Simulation results illustrate that the multiple transmitter–detector pairs can potentially resolve fluorescent images from the scattering and multiphoton fluorescence, and give 3D information.

[1] W. Denk, J. H. Strickler, and W. W. Webb, Science **248**, 73 (1990).
[2] W. G. Andrew, *Introduction to Biomedical Imaging* (Wiley, Piscataway, NJ, 2002).
[3] J. Ryu, S. S. Hong, B. K. P. Horn, D. M. Freeman, and M. S. Mermelstein Appl. Phys. Lett. **88**, 171112 (2006).
[4] R. Soref, Proc. IEEE **81**, 1687 (1993).
[5] D. Marris-Morini, X. L. Roux, L. Vivien, E. Cassan, D. Pascal, M. Halbwax, S. Maine, S. Laval, J. M. Fedeli, and J. F. Damlencourt, Opt. Express **14**, 10838 (2006).
[6] N. Yao and Z. L. Wang, *Handbook of Microscopy for Nanotechnology* (Kluwer, Boston, 2005).
[7] O. Boyraz and B. Jalali, Opt. Express **12**, 5269 (2004).
[8] E. K. Tien, F. Qian, N. S. Yuksek, and O. Boyraz, Appl. Phys. Lett. **91**, 201115 (2007).
[9] G. K. Celler and S. Cristoloveanu, J. Appl. Phys. **93**, 4955 (2003).
[10] H. S. Rong, R. Jones, A. S. Liu, O. Cohen, D. Hak, A. Fang, and M. Paniccia, Nature (London) **433**, 725 (2005).
[11] S. Fathpour, K. K. Tsai, and B. Jalali, IEEE J. Quantum Electron. **43**, 1211 (2007).
[12] E. Lorenzo, G. L. Araújo, A. Cuevas, M. Egido, J. Minano, and R. Zilles, *Solar Electricity* (Earthscan, Madrid, 1994).
[13] V. Krishnamurthi, Y. H. Liu, S. Bhattacharyya, J. N. Turner, and T. J. Holmes, Appl. Opt. **34**, 6633 (1995).
[14] P. Sarder and A. Nehorai, IEEE Signal Process. Mag. **23**, 32 (2006).
[15] S. Saladi, P. Pinnamaneni, and J. Meyer, Proceedings of the IEEE Second International Symposium on Bioinformatics and Bioengineering Conference, Bethesda, MD, 4–6 November 2001 (unpublished), Vol. 4, p. 136.